Biotic−Abiotic Interactions: Factors that Influence Peptide−Graphene Interactions

Steve S. Kim, Zhifeng Kuang, Yen H. Ngo, Barry L. Farmer, and Rajesh R. Naik*

Materials and Manufacturing Directorate, Air Force Research Laboratory, Wright-Patterson Air Force Base, Ohio 45433, United States

ⓢ Supporting Information

ABSTRACT: Understanding the factors that influence the interaction between biomolecules and abiotic surfaces is of utmost interest in biosensing and biomedical research. Through phage display technology, several peptides have been identified as specific binders to abiotic material surfaces, such as gold, graphene, silver, and so forth. Using graphene−peptide as our model abiotic−biotic pair, we investigate the effect of graphene quality, number of layers, and the underlying support substrate effect on graphene−peptide interactions using both experiments and computation. Our results indicate that graphene quality plays a significant role in graphene−peptide interactions. The graphene−biomolecule interaction appears to show no significant dependency on the number of graphene layers or the underlying support substrate.

KEYWORDS: graphene, peptides, molecular interactions, QCM, molecular dynamics, phage display
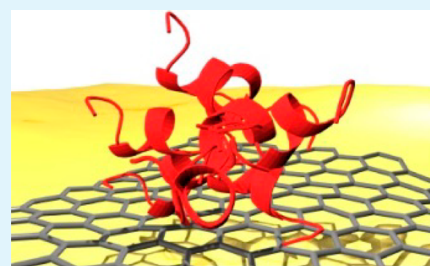
INTRODUCTION

Graphene is a zero-bandgap, two-dimensional (2D) semiconducting material with extremely high electron/hole mobility in the ballistic transport regime.[1−3] The superior electronic, thermal, and mechanical properties of the 2D atomically thin graphene have attracted significant attention in the development of high performance nanoelectronics. The electronic properties of graphene are highly sensitive to the surrounding environment and can be exploited for sensing applications using graphene field effect transistors (GFETs) for the ultrasensitive detection of biological and chemical species.[4−6] A typical graphene device platform is based on single- or double-layer graphene that is supported by an underlying support substrate, such as a SiOx/Si wafer. Recent studies have shown that the physicochemical properties of single/few layer graphene can be influenced by both the support substrates and the adsorbates.[7−9] For example, the electronic properties of graphene can be affected by changing the amino acid composition of a graphene binding peptide.[9]

Biological recognition elements (BREs) such as antibodies, peptides, and nucleic acids immobilized onto the graphene sensor surface are able to specifically capture the target molecule, thereby causing a change in the electronic properties of graphene. A number of functionalization approaches, noncovalent and covalent chemistries, have been developed to immobilize the BREs onto graphene surfaces. Recent studies have demonstrated the use of noncovalent biological interactions to specifically functionalize graphene for biosensing applications.[4,10] The noncovalent peptide multifunctional BREs are designed to play a role as a "bridge" between the target molecule and the graphene device surface.[5,10] The peptides selected from peptide combinatorial libraries have been shown

to be capable of selectively binding to the edge of planar graphene surfaces as well.[10,11] An in-depth understanding of factors that influence the interaction between the biotic component and abiotic graphene surface is of great importance in performance optimization of nanoelectronic graphene biosensors. In this study, we investigate the role of the abiotic component graphene and its interaction with the biotic component. Specifically, we examine the recognition of graphene by peptides with respect to the quality of graphene, number of graphene layers, and underlying substrate support. Our results indicate that the binding of peptides to the graphene surface in aqueous media strongly depends on the quality of graphene and is not influenced by the number of graphene layers or the underlying support substrate. We further explore the peptide−graphene−substrate biotic−abiotic interaction using molecular dynamic simulations. Although peptides can interact with solid substrates via hydrophobic interactions, hydrogen bonding, electrostatics, and van der Waals (vdW) forces, the vdW interaction energy (IE) profile shows that the graphene−peptide interaction does not depend on the supporting gold surface or the number of graphene layers, consistent with our experimental results. The influence of these factors on the noncovalent interaction between graphene and a peptide binder can be used to modulate the performance of graphene-based bioelectronics devices.
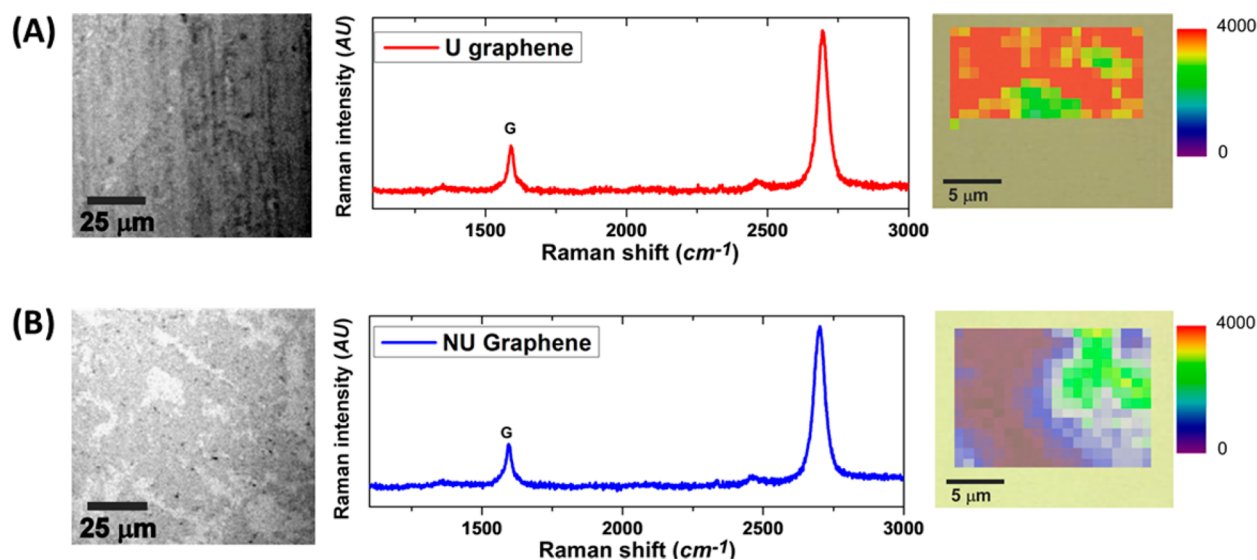
Figure 1. Optical micrograph, RRS, and graphene RRS G-intensity mapping image from CVD grown (A) U- and (B) NU-graphene on a silicon wafer substrate.

■ EXPERIMENTAL SECTION

Peptides. CBP (-HSSYWYAFNNKT-), GBP (-EPLQLKM-), and A3 (-AYSSGAPPMPPF-) peptides (>95% purity) were custom synthesized from Peptide 2.0 Inc. (Chantilly, VA). Peptide solutions (0.02 mg/mL) were prepared in double distilled deionized (DI) water. All of the peptide solutions and experiments were performed using DI water unless stated otherwise.

Graphene Growth and Processing. A tube furnace (OTF-1200x-S, MTI Corporation, CA) equipped with a scroll vacuum pump was used for graphene chemical vapor deposition (CVD). A 4×4 in^2 copper foil was placed in the furnace and heated to 1000 °C while a hydrogen flow was injected at a pressure of 125 mTorr. The hydrogen-only reduction step continued for 30 min at 1000 °C. Then, a methane gas was flowed at a pressure of 1.25 Torr for 30 min at 1000 °C. The furnace was powered off and allowed to cool to room temperature while keeping the flow of methane and hydrogen. Graphene grown on the Cu foil was transferred to a thermal release (TR) tape (Nitto Americas Inc., CA). A TR tape was carefully placed over the graphene-coated copper film to prevent any air bubbles from being entrapped. This was followed by a 5 min oxygen plasma treatment on the Cu side at 35 mW. For uniform (U) graphene, the Cu on tape was etched with $(NH_4)_2S_2O_8$ (100 mg/mL in DI water) for 3 h, rinsed with DI water, and dried by blowing nitrogen. For nonuniform (NU) graphene, the Cu on tape was etched with $Fe(NO_3)_3$ etchant (50 mg/mL DI water) overnight, rinsed with DI water, and dried by blowing nitrogen. Graphene-TR tape was adhered to various substrates at room temperature, then peeled off upon heating on a 125 °C hot plate, leaving mostly a single layer of graphene on the substrate. The transfer process was repeated over again for multilayer graphene. Forming gas (H_2/Ar) was used to further anneal the transferred CVD graphene at 345 °C for 4 h to reduce the adsorbed organic and TR tape residues while keeping the graphene structurally intact.

Resonance Raman Spectroscopy (RRS). RRS spectra were obtained using a Renishaw inVia Raman microscope equipped with a 2.32 eV excitation laser focused with a 50× objective. All samples were subjected to the same laser intensity, exposure time, and accumulation number. The full range RRS were collected and averaged from 30 spots to avoid spot-by-spot spectral variance.

Quartz Crystal Microbalance (QCM). All QCM measurements were performed using Q-sense E4 and resonators purchased from Biolin Scientific (Sweden). Mass deposition was measured using quartz crystal sensors (resonators) with 40–1000 nm metal/metal oxide electrode coatings with root-mean-square surface roughnesses of <3 nm. Quartz crystal sensors were cleaned prior to use with a 5 min ozone-UV treatment. This was followed by 30 min DI water, 30 min 2 wt % sodium dodecyl sulfate (SDS) solution, and 30 min DI water at a 0.350 mL/min flow rate in the QCM instrument. To establish a stable baseline, we injected DI water into the QCM cell for 5–10 min before flowing 0.170 µL/min of peptide solutions. All QCM measurements were performed in triplicate. The change in oscillation frequency (f) is directly related to the adsorbate mass on the electrode surface using a simplified Sauerbrey relationship, $\Delta m = -C_{QCM} (\Delta f_n/n)$, where Δm, C_{QCM}, and Δf_n are the adsorbate mass, the mass sensitivity constant (17.7 ng/cm^2/s), and the frequency change at the nth overtone, respectively.

Water Contact Angle (WCA) Measurements. After cleaning the substrates to an adsorbate-free surface using high temperature annealing or ozone treatment, the samples were incubated in ambient air for 60–120 min to ensure that the WCA was stable from airborne contaminants.[12] The WCA was measured by monitoring a sessile drop profile using a Theta optical tensiometer (Biolin Scientific, Sweden) with OneAttension analysis software. Young–Laplace analysis mode was used to estimate WCA from DI water with a drop out size of 3 µL. All of the tests were carried out in triplicate at room temperature in ambient air.

Molecular Dynamics (MD) Simulation. A (111) gold surface of size 7.11 nm × 7.03 nm × 1.06 nm was used as the substrate. One, two, three, and four layers of graphene sheets matching gold substrate dimensions were evenly stacked on the underlying gold substrate with a separation distance of 0.35 nm as the starting configuration. Bonds across the periodic boundaries of graphene sheets were made following VMD Bionanotechnology Tutorial (http://www.ks.uiuc.edu/Training/Tutorials/) such that infinite graphene sheets were simulated using periodic conditions. The previously equilibrated CBP peptide structure adsorbed on graphene sheets was transferred above the simulated surfaces.[13] One chloride ion is used to neutralize the positive charge from lysine. The system is solvated in 10625 TIP3 water. The recently developed polarizable force field GolP for gold and protein interactions in water is used in all simulations. The van der Waals (vdW) parameters for benzene carbon type were used to describe the carbon atoms in graphene sheets. The combination of GolP and parameters for proteins in NAMD format are kindly provided by Bellucci.[14−17] All structures are constructed using VMD.[18] All molecular dynamics simulations are performed using NAMD.[19] A nonbonded cutoff distance of 1.0 nm is used with the application of the switching function starting at 0.9 nm. Periodic boundary conditions are applied in all three dimensions. First, the system was minimized using a sophisticated conjugate gradient and line search algorithm. Second, the system was gradually heated to 300 K from 0 K by increasing the temperature 30 K every 1000 steps. Third, the

system was equilibrated for 45 ns. Finally, the pairwise interaction energy was calculated using the last 5 ns of the trajectory.

■ RESULTS AND DISCUSSION

The characterization of biomolecular binding on single atomic layer graphene using conventional macroscale instruments has been primarily limited by the lack of quality-controlled large scale graphene preparation processes. However, the development of CVD graphene synthesis[20] and transfer[21] technology enables one to fabricate consistently large area graphene on various substrates. Large area graphene is typically CVD grown on mostly nickel or copper metal foils, and postgrowth processing techniques are used to selectively etch away the underlying metal and for the transfer of graphene onto a supporting substrate.[22] A recent study demonstrated a method to obtain large scale CVD grown graphene with superior quality having comparable mechanical toughness to ablated crystalline graphene obtained from bulk graphite.[23] An aqueous ammonium persulfate-etching process of Cu foil was found to be a key component in producing defect-free and tough graphene in contrast to the commonly used ferric nitrate etchant.[23] Following this earlier study, we obtained large-area CVD graphene using either ammonium persulfate or ferric nitrate for etching the Cu foil (Figure 1). The optical micrograph from our CVD grown graphene on silicon wafer substrates shows that the ammonium persulfate-etching yields relatively large areas of void-free uniform graphene (U-graphene, Figure 1A). In contrast, the ferric nitrate etchant results in nonuniform graphene (NU-graphene) with areas void of graphene with dimensions of a few to 10s of micrometers (Figure 1B). Consistent with observations from previous work,[23] the localized resonance Raman spectra (RRS) D, G, and 2D peaks indicate that the atomic level quality of graphene appears to be identical for both samples. In contrast, large area spectral mapping of the G-band intensity shows a stark contrast between the U- and NU-graphene. The characteristic G-band intensity mapping is more uniformly present for the ammonium persulfate etched U-graphene than the ferric nitrate etched NU-graphene. Surveying a large area of the graphene surface with RRS mapping and microscopy, rather than just relying on the localized RRS spectra, is critically important in the assessment of sample quality.

Next, we probed the binding characteristics of peptides to the U- and NU-graphene using QCM, which is a useful technique to monitor the affinity of molecules for a surface by monitoring the change in resonance frequency of a quartz crystal during and after their physisorption or chemisorption.[24,25] The resonant frequency of the piezoelectrically excited AT-cut QCM is sensitive to the amount of material mass adsorbed on the crystal surface. The accumulating mass changes derived from the frequency change provide valuable real-time information on the adsorption of molecules. Graphene-coated QCM resonators are prepared by transferring similarly sized single or multiple layer U- or NU-graphene sheets onto the electrode-covered sensing side of the quartz crystals. The U- and NU-graphene-coated QCM resonators enable us to test the effect of the quality of graphene on peptide binding. The binding of our previously described graphene planar binding peptide (CBP) and graphene edge binding peptide (GBP) are mostly tested to U- or NU-graphene coatings in this study. The mass profile obtained from 0 to 8 L U-graphene coating on QCM resonating sensor (Figure S1) shows linearity with respect to the number of graphene layers, ensuring that

repetitive graphene transfer is a reliable process. It is notable that the linear fit 89.1 ng/cm^2/layer U-graphene shown in Figure S1 is in close proximity to a theoretical single layer graphene aerial weight of 76.1 ng/cm^2.

The representative QCM profiles obtained from the resonance crystals covered with 0−8 layers of U- or NU-graphene for the adsorption of graphene-plane binding peptide CBP (0.02 mg/mL) is shown in Figure 2. It is notable that U-
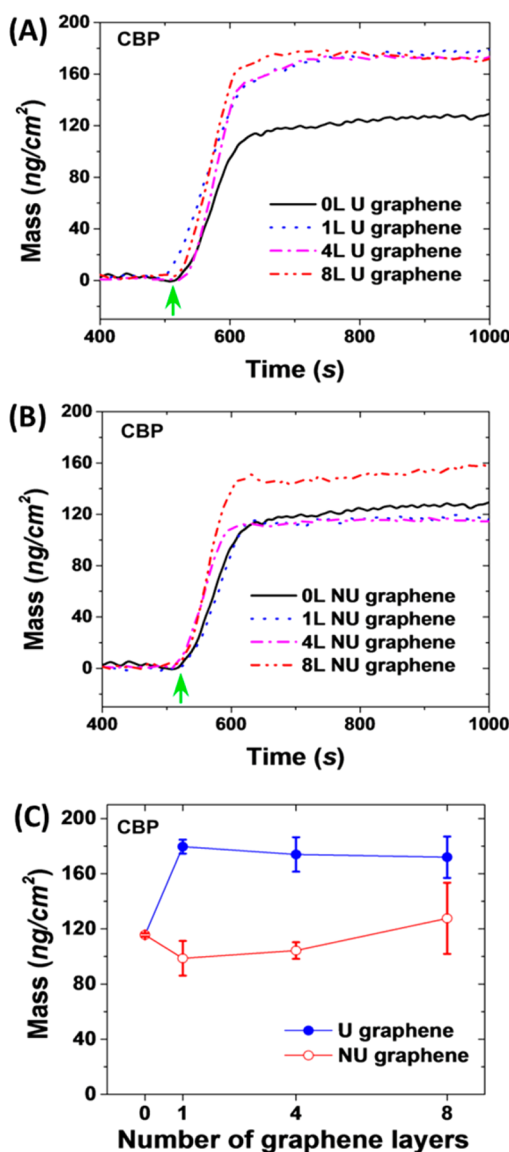

Figure 2. Adsorption of CBP to graphene. The adsorbed mass of CBP to QCM resonators coated with (A) U- and (B) NU-graphene. Arrows indicate the injection point of the peptide solution. (C) Adsorbed CBP mass vs the number of U- or NU-graphene layers.

graphene (Figure 2A) shows an increase in the accumulating mass due to CBP binding to single layer graphene (180 ng/cm^2) as compared to that of the bare gold QCM electrode (115 ng/cm^2). The accumulative mass of CBP stays close to 180 ng/cm^2 even after the number of U-graphene layers is increased to 4 or 8 layers. In contrast, 1- and 4-layer NU-graphene show decreases in accumulating CBP mass as compared to that of the bare gold QCM. Then, the 8-layer NU-graphene exhibits a moderate increase to ~130 ng/cm^2 (Figure 2B). The increase

in the mass with 8-layer NU-graphene is most likely due to the masking of voids/defects by the additional graphene layers. The mass accumulation profile obtained from triplicate QCM measurements shows that CBP consistently binds more to single-/multilayer U-graphene than to single-/multilayer NU-graphene (Figure 2C). This indicates that the surface coverage of CBP is dependent on uniformity/quality of the graphene samples. Overall, these results suggest that the graphene quality should be considered as a critical factor in probing the interaction of graphene with adsorbing molecules.

Atomic force microscopy (AFM, Figure S2) and X-ray photoelectron spectroscopy (XPS, Figure S3) were routinely used to confirm the binding of peptide to the graphene surface. The absence of Fe and Cu peaks in the XPS spectra rules out any effect on peptide binding from residual metal from the graphene growth and processing steps. The binding rate constant (K_{obs}) was calculated from real-time peptide binding characteristics obtained using a mechanically exfoliated (ME) graphene field effect transistor (GFET), CVD-GFET, and CVD graphene-coated QCM (Figure S4). The K_{obs} for CBP was 0.012, 0.011, and 0.012 s^{-1} obtained using ME-GFET, CVD-GFET, and CVD graphene-coated QCM, respectively.

Recent studies using azo-chemistry[7] and water contact angle measurements[8] on graphene have shown that the physico-chemical properties of a single/few layer graphene are influenced by the underlying supporting substrate. Wang et al. demonstrated that an embedded pattern under a graphene affects the graphene surface chemistry to the diazo compounds, enabling site-selective chemical functionalization of the graphene.[7] Rafiee et al. reported that the hydrophilicity of the supporting substrate layer transmits through a single or few layer graphene and influences the hydrophobic character of graphene.[8] Although these observations of "chemical and wetting transparency" of graphene have been investigated using nonspecific invasive chemical modification and water droplets, we wanted to examine whether such "transparency" effects influence the interaction between peptides and graphene. It is plausible that if the surface energy of graphene is influenced by the underlying substrate, this in turn can influence its interaction with biomolecules. However, the accumulation of CBP reaches saturation with a single layer of U-graphene in our data, suggesting that the single layer graphene does not exhibit substrate transparency when interacting with the graphene binding peptide. If this hypothesis holds, using void-free single atomic layer U-graphene should effectively screen off any effect of the underlying substrate on peptide adsorption, and the interaction will be dominated by the top graphene layer irrespective of the underlying support substrate. We tested this hypothesis using QCM resonators coated with various inorganic metals or metal oxides, such as Cu, TiO$_2$, and SiO$_2$ (Figure 3). These metal and metal oxide-coated QCM crystals overlaid with 0–8 layers of U-graphene were used to examine peptide adsorption to graphene. All of the inorganic-coated substrates examined show similar CBP binding characteristics as those of the bare Au resonators. Regardless of the underlying substrate, the single layer U-graphene overlaid onto Cu-, TiO$_2$-, and SiO$_2$-coated QCM resonators shows that CBP assembles on it to a similar accumulative mass. Increasing the number of graphene layers appears to have no further noticeable impact on CBP adsorption. Together, these results suggest that the screening of any underlying substrate effect can be achieved by a single layer graphene, and graphene transparency toward the
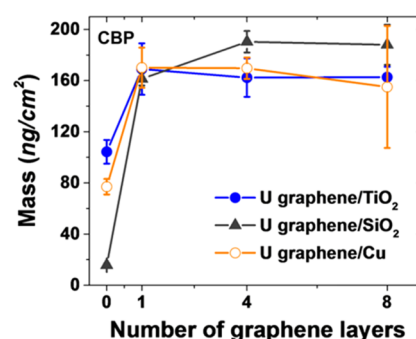

Figure 3. CBP mass adsorbed onto U-graphene deposited on TiO$_2$-, SiO$_2$-, or Cu-coated QCM resonators.

underlying substrate is not observed with respect to peptide adsorption. In other words, the molecular recognition and binding of the peptide to graphene do not appear to be influenced by the underlying support substrate.

Graphene-edge binding peptide (termed GBP) specifically accumulating at graphene edges was also studied for its binding to U- and NU-graphene.[11] The binding area for GBP, graphene edges, is much smaller than the available planar binding area for CBP with CVD-grown graphene. Thus, smaller mass accumulation on U-graphene by GBP compared to that by CBP is expected. However, we speculate as to whether GBP binding behavior is impacted by NU- versus U-graphene (Figure 4A−C). The mass accumulation of GBP to a bare gold-coated QCM crystal is similar to that of CBP (~105 ng/cm^2). However, upon coating the QCM with a single layer of U-graphene, the binding of GBP decreases significantly and stays relative constant (~40 ng/cm^2) even upon increasing the number of U-graphene layers (Figure 4A). GBP-binding to 1- or 4-layer NU-graphene is higher than to U-graphene because these samples most likely have a larger number of edges and defects (Figure 4B). Any quantitative evaluation of the number of edges or defect sites on the CVD graphene is limited at present. However, multiple QCM experiments performed using NU-graphene show larger variation in GBP adsorption, unlike U-graphene, which shows relatively constant mass accumulation (Figure 4C). These results further lend support to the need for controlling graphene quality when probing the graphene−peptide interactions.

As a control experiment for our QCM studies, we performed similar experiments on peptide adsorption using an A3 gold-binding peptide (-AYSSGAPPMPPF-).[26] The A3 peptide has been previously shown to have a high affinity toward gold surfaces. Hence, the A3 peptide should bind strongly to the gold-coated QCM resonator relative to that of the one overlaid with graphene. As shown in Figure 5, the accumulative mass change of the A3 peptide for a bare QCM (Au-only surface) decreases by ~3 fold when the resonator surface is covered with a single U-graphene layer. Very little change in peptide adsorption is observed even with 4- or 8-layer graphene. Together, this experiment suggests that the A3 peptide loses its affinity for the gold surface when overlaid with even a single graphene layer and again highlights the absence of graphene-transparency for the A3 peptide binding. This further lends support to our earlier result that CBP recognizes the graphene layer and not the underlying substrate.

We further explored the peptide−graphene−substrate relationship using molecular dynamic simulations. Peptides are charged macromolecules that can interact with solid
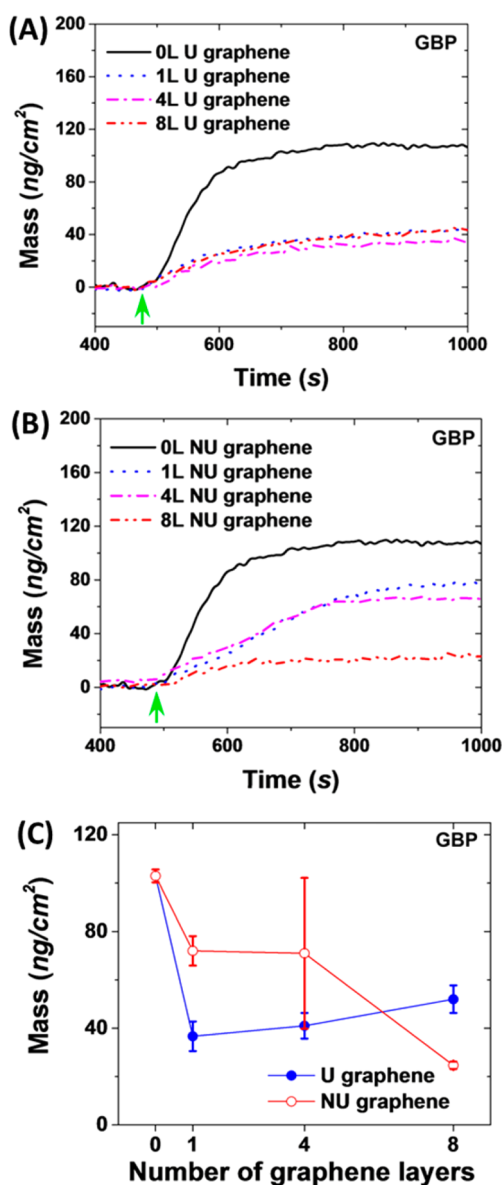
Figure 4. Adsorption of GBP to graphene. The adsorbed mass of GBP to QCM resonators coated with (A) U-graphene and (B) NU-graphene. Arrows indicate the injection point of the peptide solution. (C) Adsorbed GBP mass vs number of U- or NU-graphene layers.
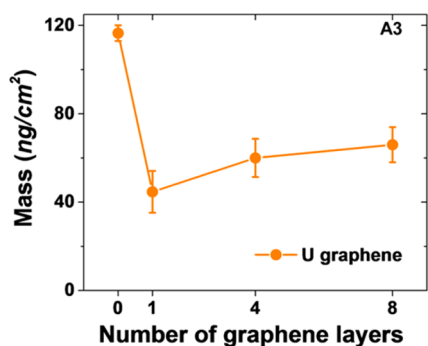

Figure 5. Gold-binding A3 peptide mass adsorbed on QCM crystal coated with 0−8 layers of U-graphene.

substrates via electrostatic and vdW forces. Because the interaction between peptide charges and substrate dipoles due

to polarizability is a longer range interaction than that between water dipoles and substrate dipoles, one would expect significant substrate effects on the peptide adsorption. However, the mass adsorption of CBP measured by QCM shows that the peptide adsorbed mass has little dependence on the underlying substrate and number of graphene layers for the uniform graphene sheets. To gain insight into these experimental results, we have resorted to MD simulations to calculate the adsorption free energy of the CBP peptide adsorbed on bare Au{111} substrate and on 1- to 4-layer graphene sheets (1−4L) supported by a Au{111} substrate. Four systems, including bare gold surface and mono-, di-, tri-, and quadruple-layer graphene-coated gold surface are simulated in explicit water. The recently developed polarizable force field GolP[16] specific for gold and protein interactions are used in our simulations. Simulations using different initial velocities are performed to obtain equilibrated configurations, and a representative simulated system is shown in Figure 6A. The time evolution of the radius of gyration of our simulated systems is shown in Figure 6B over a 45 ns simulation time. To estimate the energetic contributions from different components, we decoupled the pairwise interaction energy into three components: the van der Waals IE between individual amino acid residues (in CBP) and gold (vdW−CBP−Au), the electrostatic IE between individual amino acid residues and gold (ES−CBP−Au), and van der Waals IE between individual amino acid residues and the top graphene sheet (vdW−CBP−graphene, see Table S1). The overall IE change for the three components with respect to the number of graphene layers is shown in Figure 6C. When the bottom gold surface is covered with 1−4 L graphene layers, the IEs for ES−CBP−Au and vdW−CBP−Au diminish, and the IE for vdW−CBP−graphene emerges. Moreover, all of the energetic contributions between the individual amino acid residues and the top graphene sheet appear to be similar, indicating that the peptide affinity to the graphene surface is not found to be dependent on the number of graphene layers. These computational results indicate that the vdW interaction driven peptide−graphene adsorption in water does not depend on the supporting gold surface or the number of graphene layers, consistent with our experimental results where the accumulative peptide mass adsorption remains relatively constant after overlaying the QCM resonator with additional layers of graphene.

The quality of graphene can also be impacted by the exposure of graphene to the ambient environment. Li and co-workers demonstrated that exposure of graphene to ambient air significantly changed the surface energy of graphene as demonstrated by a change in the water contact angle (WCA) from ∼45° to ∼80°.[12] This hydrophilic to hydrophobic transformation of the graphene surface was attributed to airborne contaminant adsorption. A similar study in our laboratory also shows that WCA changes from 25° to 80° upon increasing the air-exposure time of U-graphene samples (Figure 7). This increase in hydrophobicity can be attributed to the ambient air contaminants in our laboratory environment. On the basis of these observations, we sought to determine the impact of exposure of graphene to ambient atmosphere on the peptide−graphene interaction. We exposed the single layer U-graphene to ambient atmosphere, measured the WCA as well as examined peptide adsorption following air exposure for varying amounts of time. The ambient atmosphere exposure of single layer U-graphene for as much as 20 h does not result in any noticeable change in CBP adsorption even though we observed
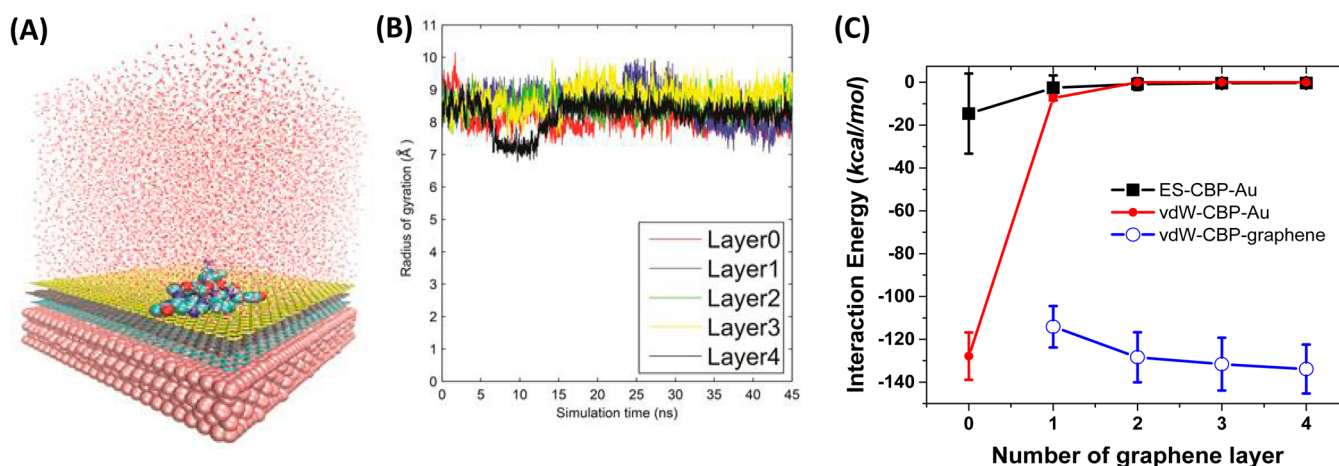
Figure 6. (A) Representative model for the CBP peptide adsorbed onto the Au{111} gold surface in water. (B) Time evolution of the radius of gyration of the CBP. (C) Overall interaction energy profile for the CBP with respect to the number of graphene layers.
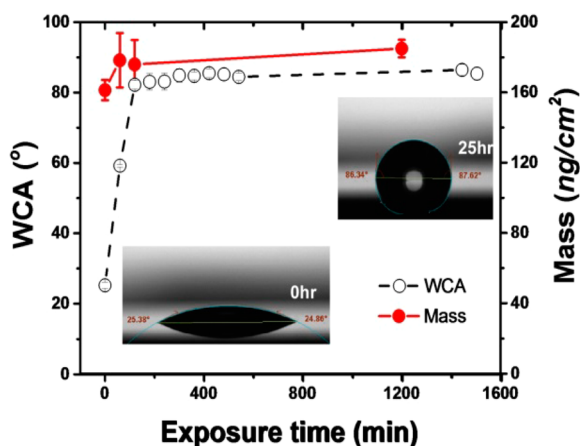

Figure 7. Water contact angle (WCA) vs exposure time to airborne contaminants in ambient atmosphere for a single layer U-graphene supported on a Si wafer. CBP adsorption mass on a single layer U-graphene after indicated exposure obtained using QCM.

a substantial change in the WCA (Figure 7). This study indicates that (1) the recognition of the graphene surface by CBP is unaffected by already adsorbed airborne contaminants and/or (2) CBP competes off any surface bound airborne adsorbates.

Overall, the studies presented here provide evidence that recognition and binding of CBP to graphene is influenced by the quality of graphene and not by the number of graphene layers or the underlying supported substrates. Furthermore, we have painstakingly tried to control the quality, number of graphene layers, and the overall size of the graphene layers transferred onto the QCM resonator. However, our studies do have limitations due to technical challenges that in general are yet to be resolved. For example, obtaining completely contaminant-free CVD graphene is still a challenging issue,[27] sporadic double or multilayer graphene islands appear to consistently exist in large scale CVD grown graphene, and the ability to accurately measure the graphene surface area is a nontrivial task. Future work on achieving contaminant- and multilayer-free large scale graphene processing would be necessary to provide greater insight into the biomolecule−graphene biotic−abiotic interaction. Moreover, the demonstration of solvent effect having a direct influence on the

binding enthalpy and entropy is expected to provide further in-depth understanding of the peptide−graphene interaction as well.[28]

CONCLUSIONS

Biomolecules that specifically recognize an abiotic surface provide a unique route for controlling interfacial properties in the context of biosensor and biomedical implant design. Phage display techniques have resulted in the identification of peptides that can specifically recognize materials.[5,26,29,30] Our study examining the interaction between peptides and graphene contributes to our understanding of biotic and abiotic interactions. We show that biomolecule−graphene interactions are influenced by the quality of graphene and that the binding of peptides to the graphene surface in aqueous media strongly depends on the graphene−peptide interaction rather than graphene−substrate interactions or the number of graphene layers. Furthermore, this study underscores the need for well-characterized materials and surfaces for studying the interaction of biomolecules and abiotic surfaces.

ASSOCIATED CONTENT

Ⓢ Supporting Information

The Supporting Information is available free of charge on the ACS Publications website at DOI: 10.1021/acsami.5b06434.

> Experimental details and additional data on QCM, AFM, XPS, and GFET measurements on peptide−graphene samples and detailed IE table obtained from MD simulations (PDF)

AUTHOR INFORMATION

Corresponding Author

*E-mail: rajesh.naik@us.af.mil.

Notes

The authors declare no competing financial interest.

■ REFERENCES

(1) Novoselov, K. S.; Geim, A. K.; Morozov, S. V.; Jiang, D.; Zhang, Y.; Dubonos, S. V.; Grigorieva, I. V.; Firsov, A. A. Electric Field Effect in Atomically Thin Carbon Films. *Science* **2004**, *306*, 666−669.

(2) Bolotin, K. I.; Sikes, K. J.; Jiang, Z.; Klima, M.; Fudenberg, G.; Hone, J.; Kim, P.; Stormer, H. L. Ultrahigh Electron Mobility in Suspended Graphene. *Solid State Commun.* **2008**, *146*, 351−355.

(3) Baringhaus, J.; Ruan, M.; Edler, F.; Tejeda, A.; Sicot, M.; Taleb, I.; Li, A.-P.; Jiang, Z.; Conrad, E. H.; Berger, C.; Tegenkamp, C.; de Heer, W. A. Exceptional Ballistic Transport in Epitaxial Graphene Nanoribbons. *Nature* **2014**, *506*, 349−354.

(4) Lerner, M. B.; Matsunaga, F.; Han, G. H.; Hong, S. J.; Xi, J.; Crook, A.; Perez-Aguilar, J. M.; Park, Y. W.; Saven, J. G.; Liu, R.; Johnson, A. T. C. Scalable Production of Highly Sensitive Nanosensors Based on Graphene Functionalized with a Designed G Protein-Coupled Receptor. *Nano Lett.* **2014**, *14*, 2709−2714.

(5) Cui, Y.; Kim, S. N.; Jones, S. E.; Wissler, L. L.; Naik, R. R.; McAlpine, M. C. Chemical Functionalization of Graphene Enabled by Phage Displayed Peptides. *Nano Lett.* **2010**, *10*, 4559−4565.

(6) Kuila, T.; Bose, S.; Khanra, P.; Mishra, A. K.; Kim, N. H.; Lee, J. H. Recent Advances in Graphene-Based Biosensors. *Biosens. Bioelectron.* **2011**, *26*, 4637−4648.

(7) Wang, Q. H.; Jin, Z.; Kim, K. K.; Hilmer, A. J.; Paulus, G. L. C.; Shih, C.-J.; Ham, M.-H.; Sanchez-Yamagishi, J. D.; Watanabe, K.; Taniguchi, T.; Kong, J.; Jarillo-Herrero, P.; Strano, M. S. Understanding and Controlling the Substrate Effect on Graphene Electron-Transfer Chemistry via Reactivity Imprint Lithography. *Nat. Chem.* **2012**, *4*, 724−732.

(8) Rafiee, J.; Mi, X.; Gullapalli, H.; Thomas, A. V.; Yavari, F.; Shi, Y.; Ajayan, P. M.; Koratkar, N. A. Wetting Transparency of Graphene. *Nat. Mater.* **2012**, *11*, 217−222.

(9) Akdim, B.; Pachter, R.; Kim, S. S.; Naik, R. R.; Walsh, T. R.; Trohalaki, S.; Hong, G.; Kuang, Z.; Farmer, B. L. Electronic Properties of a Graphene Device with Peptide Adsorption: Insight from Simulation. *ACS Appl. Mater. Interfaces* **2013**, *5*, 7470−7477.

(10) Khatayevich, D.; Page, T.; Gresswell, C.; Hayamizu, Y.; Grady, W.; Sarikaya, M. Selective Detection of Target Proteins by Peptide-Enabled Graphene Biosensor. *Small* **2014**, *10*, 1505−1513.

(11) Kim, S. N.; Kuang, Z.; Slocik, J. M.; Jones, S. E.; Cui, Y.; Farmer, B. L.; McAlpine, M. C.; Naik, R. R. Preferential Binding of Peptides to Graphene Edges and Planes. *J. Am. Chem. Soc.* **2011**, *133*, 14480−14483.

(12) Li, Z.; Wang, Y.; Kozbial, A.; Shenoy, G.; Zhou, F.; McGinley, R.; Ireland, P.; Morganstein, B.; Kunkel, A.; Surwade, S. P.; Li, L.; Liu, H. Effect of Airborne Contaminants on the Wettability of Supported Graphene and Graphite. *Nat. Mater.* **2013**, *12*, 925−931.

(13) Kim, S. N.; Kuang, Z.; Slocik, J. M.; Jones, S. E.; Cui, Y.; Farmer, B. L.; McAlpine, M. C.; Naik, R. R. Preferential Binding of Peptides to Graphene Edges and Planes. *J. Am. Chem. Soc.* **2011**, *133*, 14480−3.

(14) Bellucci, L.; Corni, S. Interaction with a Gold Surface Reshapes the Free Energy Landscape of Alanine Dipeptide. *J. Phys. Chem. C* **2014**, *118*, 11357−11364.

(15) Iori, F.; Corni, S. Including Image Charge Effects in the Molecular Dynamics Simulations of Molecules on Metal Surfaces. *J. Comput. Chem.* **2008**, *29*, 1656−66.

(16) Iori, F.; Di Felice, R.; Molinari, E.; Corni, S. GolP: An Atomistic Force-Field to Describe the Interaction of Proteins with Au(111) Surfaces in Water. *J. Comput. Chem.* **2009**, *30*, 1465−1476.

(17) Bellucci, L.; Brancolini, G.; Calzolari, A.; Parramon, O. C.; Corni, S.; Di Felice, R. Proteins and Peptides at Gold Surfaces: Insights from Atomistic Simulations. *ACS Symp. Ser.* **2012**, *1120*, 229−250.

(18) Humphrey, W.; Dalke, A.; Schulten, K. VMD: Visual Molecular Dynamics. *J. Mol. Graphics* **1996**, *14*, 33−38.

(19) Phillips, J. C.; Braun, R.; Wang, W.; Gumbart, J.; Tajkhorshid, E.; Villa, E.; Chipot, C.; Skeel, R. D.; Kalé, L.; Schulten, K. Scalable Molecular Dynamics with NAMD. *J. Comput. Chem.* **2005**, *26*, 1781−1802.

(20) Li, X.; Cai, W.; An, J.; Kim, S.; Nah, J.; Yang, D.; Piner, R.; Velamakanni, A.; Jung, I.; Tutuc, E.; Banerjee, S. K.; Colombo, L.; Ruoff, R. S. Large-Area Synthesis of High-Quality and Uniform Graphene Films on Copper Foils. *Science* **2009**, *324*, 1312−1314.

(21) Bae, S.; Kim, H.; Lee, Y.; Xu, X.; Park, J.-S.; Zheng, Y.; Balakrishnan, J.; Lei, T.; Ri Kim, H.; Song, Y. I.; Kim, Y.-J.; Kim, K. S.; Ozyilmaz, B.; Ahn, J.-H.; Hong, B. H.; Iijima, S. Roll-to-Roll Production of 30-Inch Graphene Films for Transparent Electrodes. *Nat. Nanotechnol.* **2010**, *5*, 574−578.

(22) Lee, Y.; Bae, S.; Jang, H.; Jang, S.; Zhu, S.-E.; Sim, S. H.; Song, Y. I.; Hong, B. H.; Ahn, J.-H. Wafer-Scale Synthesis and Transfer of Graphene Films. *Nano Lett.* **2010**, *10*, 490−493.

(23) Lee, G.-H.; Cooper, R. C.; An, S. J.; Lee, S.; van der Zande, A.; Petrone, N.; Hammerberg, A. G.; Lee, C.; Crawford, B.; Oliver, W.; Kysar, J. W.; Hone, J. High-Strength Chemical-Vapor−Deposited Graphene and Grain Boundaries. *Science* **2013**, *340*, 1073−1076.

(24) Marx, K. A. Quartz Crystal Microbalance: A Useful Tool for Studying Thin Polymer Films and Complex Biomolecular Systems at the Solution−Surface Interface. *Biomacromolecules* **2003**, *4*, 1099−1120.

(25) Tamerler, C.; Oren, E. E.; Duman, M.; Venkatasubramanian, E.; Sarikaya, M. Adsorption Kinetics of an Engineered Gold Binding Peptide by Surface Plasmon Resonance Spectroscopy and a Quartz Crystal Microbalance. *Langmuir* **2006**, *22*, 7712−7718.

(26) Slocik, Joseph M.; Stone, Morley O.; Naik, Rajesh R. Synthesis of Gold Nanoparticles Using Multifunctional Peptides. *Small* **2005**, *1*, 1048−1052.

(27) Lin, Y.-C.; Lu, C.-C.; Yeh, C.-H.; Jin, C.; Suenaga, K.; Chiu, P.-W. Graphene Annealing: How Clean Can It Be? *Nano Lett.* **2011**, *12*, 414−419.

(28) Camden, A. N.; Barr, S. A.; Berry, R. J. Simulations of Peptide-Graphene Interactions in Explicit Water. *J. Phys. Chem. B* **2013**, *117*, 10691−10697.

(29) Sarikaya, M.; Tamerler, C.; Jen, A. K. Y.; Schulten, K.; Baneyx, F. Molecular Biomimetics: Nanotechnology Through Biology. *Nat. Mater.* **2003**, *2*, 577−585.

(30) Vallee, A.; Humblot, V.; Pradier, C.-M. Peptide Interactions with Metal and Oxide Surfaces. *Acc. Chem. Res.* **2010**, *43*, 1297−1306.